Agricultural and Forest Meteorology 234 (2017) 115–126

Contents lists available at ScienceDirect

Agricultural and Forest Meteorology

journal homepage: www.elsevier.com/locate/agrformet

Subterranean ventilation of allochthonous CO_2 governs net CO_2 exchange in a semiarid Mediterranean grassland

Ana López-Ballesteros[a,b,*], Penélope Serrano-Ortiz[b,c], Andrew S. Kowalski[b,d], Enrique P. Sánchez-Cañete[b,e], Russell L. Scott[f], Francisco Domingo[a]

[a] Departamento de Desertificación y Geo-ecología, Estación Experimental de Zonas Áridas (CSIC), Almería, Spain
[b] Instituto Interuniversitario de Investigación del Sistema Tierra en Andalucía (IISTA-CEAMA), Universidad de Granada, Granada, Spain
[c] Departamento de Ecología, Universidad de Granada, Granada, Spain
[d] Departamento de Física Aplicada, Universidad de Granada, Granada, Spain
[e] Biosphere 2, University of Arizona, Tucson, AZ, USA
[f] Southwest Watershed Research Center (ARS, USDA), Tucson, AZ, USA

ARTICLE INFO

Article history:
Received 19 July 2016
Received in revised form 3 December 2016
Accepted 26 December 2016

Keywords:
Net CO_2 flux
Advective transport
Eddy covariance
Vadose zone
Drought
Atmospheric pumping

ABSTRACT

Recent research highlights the important role of (semi-)arid ecosystems in the global carbon (C) cycle. However, detailed process based investigations are still necessary in order to fully understand how drylands behave and to determine the main factors currently affecting their C balance with the aim of predicting how climate change will affect their structure and functions. Here, we explore the potential biological and non-biological processes that may compose net CO_2 exchange in a semiarid grassland in southeast Spain by means of eddy covariance measurements registered over six hydrological years (2009–2015). Results point out the great importance of subterranean ventilation, an advective transport process causing net CO_2 release, especially during drought periods and under high-turbulence conditions. Accordingly, extreme CO_2 release, far exceeding that found in the literature, was measured over the whole study period (2009–2015) averaging 230 g C m^{-2} $year^{-1}$; this occurred mostly during the dry season and was very unlikely to correspond to concurrent biological activity and variations of *in situ* organic C pools. Underground CO_2 concentrations corroborate this finding. In this regard, the potential origins of the released CO_2 could be geological degassing and/or subterranean translocation of CO_2 in both gaseous and aqueous phases. However, future research is needed in order to understand how CO_2 transport and production processes interact and modulate drylands' terrestrial C balance. Overall, the present study exposes how subterranean ventilation and hydrogeochemistry can complicate the interpretation of the terrestrial C cycle.

1. Introduction

Anthropogenic emissions of carbon dioxide (CO_2) have been rising since the beginning of the industrial era, increasing concentrations from 277 parts per million (ppm) to approximately 400 ppm (Dlugokencky and Tans, 2014; Joos and Spahni, 2008). The major role of the biosphere as a natural CO_2 sink is extensively known given that the oceans and terrestrial ecosystems combined remove around 50% of the anthropogenically emitted CO_2 (Le Quéré et al., 2009). Thus, it is crucial to understand the processes, feedbacks and driving factors that modulate the carbon (C) sink capacity of natural ecosystems given their implications for future climate. In this context, recent studies have determined that drylands' C balance strongly affects the inter-annual variability of C dynamics at a global scale (Ahlström et al., 2015; Metcalfe, 2014; Poulter et al., 2014). Hence, given the wide presence of arid and semiarid ecosystems (Okin, 2001; Schlesinger, 1990), more research is needed in order to understand how these ecosystems behave, in terms of processes and climatic forcing factors that are involved in their C cycle.

During the last decade, research related to drylands' C balance has demonstrated that biological processes, such as photosynthesis and plant and soil respiration, occasionally play a secondary

* Corresponding author at: Departamento de Desertificación y Geo-ecología, Estación Experimental de Zonas Áridas (CSIC), Almería, Spain.
E-mail addresses: alpzballesteros@gmail.com (A. López-Ballesteros), penelope@ugr.es (P. Serrano-Ortiz), andyk@ugr.es (A.S. Kowalski), epsanchezcanete@email.arizona.edu (E.P. Sánchez-Cañete), Russ.Scott@ars.usda.gov (R.L. Scott), poveda@eeza.csic.es (F. Domingo).

http://dx.doi.org/10.1016/j.agrformet.2016.12.021
0168-1923/

Table 1
Variables measured, sensors used and their installation height in Amoladeras experimental site.

Variable	Sensor	Sensor height
	Eddy Covariance system	
Wind speed (3-D) and sonic temperature	A three-axis sonic anemometer (CSAT-3, Campbell Scientific, Logan, UT, USA)	3.05 m
CO_2 and H_2O vapor densities	A open-path infrared gas analyzer (Li-Cor 7500, Lincoln, NE, USA)	3.05 m
	Meteorological soil and vadose zone measurements	
Air pressure	A open-path infrared gas analyzer (Li-Cor 7500, Lincoln, NE, USA)	3.05 m
Photosynthetic photon flux density	Two PAR sensors (Li-190, Li-Cor, Lincoln, NE, USA)	1.40 m
Net radiation	A net radiometer (NR Lite, Kipp&Zonen, Delft, Netherlands)	1.70 m
Air temperature	A thermohygrometer (HMP35-C, Campbell Scientific, Logan, UT, USA)	3.62 m
Air relative humidity	A thermohygrometer (HMP35-C, Campbell Scientific, Logan, UT, USA)	3.62 m
Rainfall	A tipping bucket (0.2 mm) rain gauge (785 M, Davis Instruments Corp., Hayward, CA, USA)	1.30 m
Soil water content	Four water content reflectometers (CS616, Campbell Scientific, Logan, UT, USA)	−0.04 m
Soil temperature	Four soil temperature probes (TCAV, Campbell scientific, Logan,UT, USA)	−0.02 and −0.06 m
Soil heat flux	Two heat flux plates (HFP01SC, Hukseflux, Delf, Netherlands)	−0.08 m
Subsoil CO_2 molar fraction	Two CO_2 sensors (GMP-343, Vaisala, Inc., Finland)	−0.15 and −1.5 m
Subsoil temperature	Two thermistors (107 temperature sensor, Campbell Scientific, Logan, UT, USA)	−0.15 and −1.5 m
Subsoil water content	Two reflectometers (CS616, Campbell Scientific, Logan, UT, USA)	−0.15 and −1.5 m

role in the ecosystem-atmosphere CO_2 exchange (Serrano-Ortiz et al., 2012). In fact, under drought conditions when biological activity is substantially reduced, non-biological processes, such as photodegradation (Rutledge et al., 2010), geochemical weathering (Emmerich, 2003), and subterranean ventilation (Kowalski et al., 2008), may influence surface C exchanges during daytime hours. In this regard, estimates of CO_2 fluxes corresponding to photodegradation of senescent organic matter equate to 0.015 and 0.179 $\mu mol\ m^{-2}\ s^{-1}$, based on microcosm measurements under natural solar radiation (Brandt et al., 2009) and eddy covariance (EC) and chamber measurements (Rutledge et al., 2010), respectively. Likewise, short-term estimates of geochemical weathering, concretely calcite precipitation, are estimated to correspond to very low CO_2 effluxes (Hamerlynck et al., 2013; Roland et al., 2013) of *ca.* 0.05 $\mu mol\ m^{-2}\ s^{-1}$ (Serrano-Ortiz et al., 2010). In contrast, subterranean ventilation (also termed "atmospheric or pressure pumping"), conceived as the advective transport of CO_2-rich air from the vadose zone to atmosphere (Sánchez-Cañete et al., 2013a,b), likely results in much more sizeable CO_2 effluxes.

Recent studies have demonstrated the relevance of subterranean ventilation for the net CO_2 exchange of some Mediterranean ecosystems. Based on EC measurements, several studies have highlighted the outstanding role of subterranean ventilation in El Llano de los Juanes, a sub-humid karstic shrubland located at Sierra de Gádor (Almería, Spain; Kowalski et al., 2008; Pérez-Priego et al., 2013; Sanchez-Cañete et al., 2011; Serrano-Ortiz et al., 2009). Likewise, significant CO_2 release was attributed to ventilation processes, especially under unstable conditions, in Balsa Blanca, a semiarid grassland located in Almería (Rey et al., 2013; Rey et al., 2012a,b; Sánchez-Cañete et al., 2013a,b). Additionally, several studies developed in temperate and alpine ecosystems also found evidence of soil ventilation induced by wind or pressure fluctuations (i.e. non-difussive gas transport) via isotope measurements (Bowling and Massman, 2011; Frisia et al., 2011), buried CO_2 sensors (Frisia et al., 2011; Hirsch et al., 2004; Maier et al., 2012, 2010; Seok et al., 2009; Takle et al., 2004), radon measurements (Fujiyoshi et al., 2009), ground-penetrating radar (Comas et al., 2007, 2011) and soil flux chambers (Redeker et al., 2015; Subke et al., 2003).

This study presents the first EC measurements of net CO_2 exchange at Amoladeras, a semiarid grassland located in SE Spain, over 2009–2015 (six hydrological years). We explore the driving biophysical processes governing the net exchange, paying special attention to subterranean ventilation whose relevance may be pronounced for this ecosystem with a very long dry season and only scant biological activity limited to the winter season. Thus, we hypothesize that the biological activity in this experimental site is constrained to very short periods when water is available, so that photosynthesis and respiration flux rates are low due to the sparse plant cover and the prolonged and extreme meteorological conditions registered over the seasonal summer drought period. Accordingly, we expect outstanding contributions from ventilation processes to the net CO_2 exchange, especially during the dry season and in the daytime hours. Our main objectives are:

1. To quantify the net CO_2 exchange at seasonal and annual scales;
2. To determine the prevalence of biological *vs.* non-biological processes in the net CO_2 exchange during growing and dry seasons over the study period (2009–2015); and
3. To quantitatively explore the magnitude of subterranean ventilation, as well as its relation with potential driving factors.

2. Material and methods

2.1. Experimental site description

The study site of Amoladeras (N36.8336°, W2.2523°; Fig. 1) is located in the Cabo de Gata-Níjar Natural Park (Almería, Spain), at an altitude of 60 m above sea level and 3.6 km from the Mediterranean Sea. The climate is dry subtropical semiarid, with a mean annual temperature of 18 °C and mean annual precipitation of approximately 220 mm. Generally, wind comes from both the Northeast and Southwest, and the wind speed is on average $3.4 \pm 2.3\ m\ s^{-1}$ over the study period. It is also characterized by a long drought period when high temperatures, absence of precipitation and high incident radiation cause a prolonged period of hydric stress, usually from May to September-October, when first rainfall events occur, after the dry season. Additionally, water inputs through dewfall episodes have been reported over all seasons in nearby experimental sites (Moro et al., 2007; Uclés et al., 2014).

The experimental site is located on an alluvial fan, where the main geological materials consist of plio-quaternary marine conglomerates and Neogene-Quaternary sediments that formed after the last volcanic events (7.5 million of years ago; Braga-Alarcón et al., 2003; Baena-Pérez et al., 1977). There is a nearby fault system, the Carboneras Fault Zone, whose last displacement in the Southern part is dated to 6 million of years ago (Rutter et al., 2012; see Appendix A in Supplementary material for more geological information). An unconfined aquifer extends 165 km^2 at approximately 50 m below the surface (Carrasco, 1988). Typical soils, classified as Calcaric Lithic Leptosol (World Reference Base for Soil Resources, 2006), are thin (0.10 m maximum), alkaline (pH above 8), and include petrocalcic horizons (Weijermars, 1991). Texture is sandy loam with sand (58.4%), silt (27%), and clay (14.5%) and with a bulk density of 1.11 $g\ cm^{-3}$. Ground cover consists of bare

Fig. 1. Amoladeras experimental site (Almería, Spain).

soil (31%), occasionally covered by biological soil crusts, gravel and rock (35%), litter (11%) and vegetation (23%). The vegetation distribution is patchy, and the main plant species are *Chamaerops humilis, Rhamnus lycoides, Pistacia lentiscus, Asparagus horridus, Olea europea* var. *sylvestris, Rubia peregrina* and *Machrocloa tenacissima,* which is clearly the most abundant. More detailed site information is given by Rey et al. (2011).

2.2. Meteorological and eddy covariance measurements

This study is based on micrometeorological data acquired by an eddy covariance (EC) tower and complementary sensors (Table 1) installed at Amoladeras (site code "Es-Amo" of the European Database Cluster (http://www.europe-fluxdata.eu) in 2009). The EC footprint is well within the fetch, even under the lowest turbulence conditions. The net CO_2, water vapor, and sensible heat fluxes were calculated from raw data collected at 10 Hz by using EddyPro 5.1.1 software (Li-Cor, Inc., USA). Data processing and quality assessment were performed according to López-Ballesteros et al. (2016). Furthermore, based on the approach proposed by Reichstein et al. (2005), the averaged u_* threshold for all the analyzed period (i.e., 2009–2015) was 0.11 m s^{-1}, which was used to filter out those measurements corresponding to low-turbulence conditions. The resulting annual fractions of missing EC flux data were 8 ± 5% and 33 ± 3% for daytime and nighttime data, respectively. The validity of our EC system was assessed via energy balance closure (Moncrieff et al., 1997). The linear regression of half-hourly turbulent energy fluxes, sensible and latent heat fluxes (H + LE; W m^{-2}) against available energy, net radiation less the soil heat flux (R_n-G; W m^{-2}), resulted in a slope of 0.873 ± 0.002 (R^2 = 0.907), which is similar to the average imbalance measured in EC systems within FLUXNET global network (i.e. 20%; Wilson et al., 2002).

2.3. Estimation of the annual cumulative CO_2 balance

Cumulative CO_2 balances, for the six hydrological years within study period (2009–2015), were estimated by integrating the half-hourly CO_2 fluxes (F_c) with quality flags equal to 0 and 1 (Mauder and Foken 2004). Missing values were gap-filled using the marginal distribution sampling technique (Reichstein et al., 2005) and random uncertainty and errors in F_c values introduced by the gap-filling process were calculated from the variance of the gap-filled data, as explained by López-Ballesteros et al. (2016). Negative values of F_c represent net CO_2 uptake while positive values denote net CO_2 emission/release to the atmosphere. In this regard, we emphasize that, in the present study, the concept of "emission" entails production and subsequent transport to the atmosphere (usually via diffusive transport) whereas "release" refers to the escape of gas to the atmosphere, regardless of when or how it has been produced.

2.4. Seasonal variability of net CO_2 exchange and driving processes

In order to analyze the time series of net CO_2 exchange at smaller time scales (i.e. seasonal) we split our database into growing and dry season periods. To do that, we chose two ambient variables, the Bowen ratio (β; ratio of sensible to latent heat fluxes) and volumetric soil water content (SWC; m^3 m^{-3}), to discern between dormancy (β > 4 and SWC ≤ 0.1) and biologically-active periods (the rest), hereinafter referred to as the dry and growing season, respectively. The same variables have been used in other Mediterranean ecosystems (Pérez-Priego et al., 2013; Serrano-Ortiz et al., 2009), but with site-adapted thresholds. Evidence that appropriate criteria were chosen is shown in Fig. 2.

Accordingly, over the growing season we explored the biological processes that presumably control the net CO_2 exchange via light-curve fitting, based on the rectangular hyperbolic model described by the following equation (Michaelis and Menten, 1913):

$$F_c = GPP_{max} \cdot PPFD / (k + PPFD) + R_d \quad (1)$$

where F_c represents daytime (R_n > 10 W m^{-2}) half-hourly net CO_2 fluxes (μmol m^{-2} s^{-1}; quality flag = 0), and the fitting coefficients are GPP_{max} (μmol m^{-2} s^{-1}), which represents gross primary productivity at infinite light, k (μmol m^{-2} s^{-1}), which is the level of Photosynthetic Photon Flux Density (PPFD; μmol m^{-2} s^{-1}) corresponding to half of the GPP_{max}, and R_d (μmol m^{-2} s^{-1}), which indicates daytime ecosystem respiration. Additionally, we studied the temperature-dependency of ecosystem respiration.

In the dry season, on the other hand, with the aim of determining the relevance of subterranean ventilation in this ecosystem, we examined the linear relationship between friction velocity (u_*), which can be viewed as a proxy for turbulence intensity, and daytime (R_n > 10 W m^{-2}) half-hourly net CO_2 fluxes (F_c; quality flag = 0), excepting those corresponding to rainfall events.

2.5. Subsoil CO_2 measurements

Subsoil CO_2, soil temperature and volumetric soil water content were measured since August 2014 within the vadose zone at 0.15 m and 1.5 m depths below the surface by means of CO_2 molar fraction sensors with soil adapters and hydrophobic filters, thermistors and water content reflectometers, respectively (Table 1). Measurements were made every 30 s and stored as 5 min averages. Missing data corresponded to 1% over the hydrological year 2014/2015. Data processing was performed according to Sánchez-Cañete et al. (2013a,b).

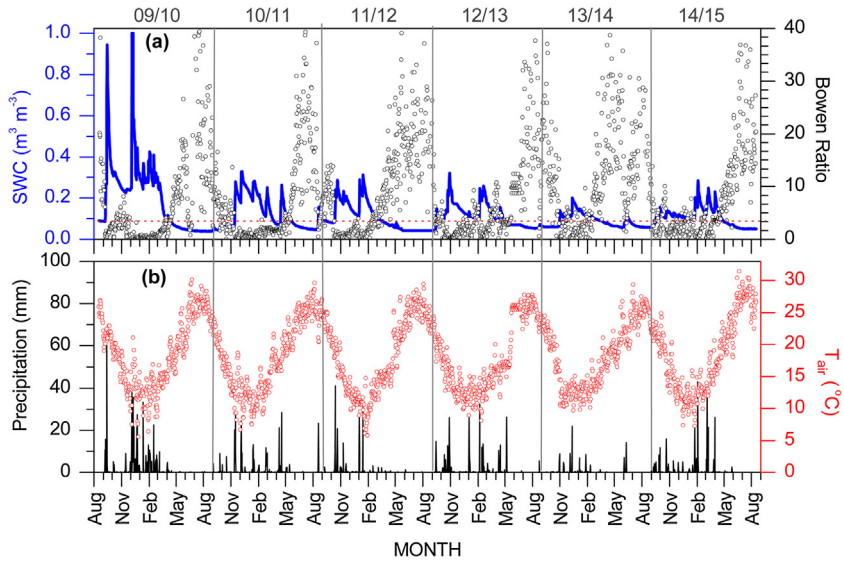

Fig. 2. Daily averaged volumetric soil water content at −0.04 m (SWC) and Bowen ratio are represented by blue line and gray dots, respectively. Threshold values for both variables used to define criteria to split data into growing and dry season are denoted by dashed red line in the upper panel. Daily precipitation (black lines) and daily averaged air temperature (T_{air}; red dots) are shown in the lower panel. (For interpretation of the references to colour in this figure legend, the reader is referred to the web version of this article.)

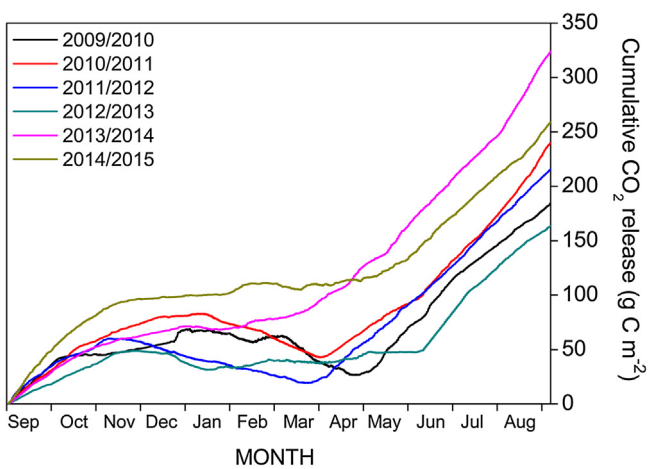

Fig. 3. Cumulative CO_2 release of every hydrological year in Amoladeras.

3. Results

3.1. Annual cumulative CO_2 release and its relationship with water availability

The six hydrological years of study showed similar air temperature (T_{air}) and Bowen ratio (β) patterns. In fact, annual averages of T_{air} ranged from 17.9 to 18.7 °C and in case of β, annual averages were between 9.4–10.7, excepting for 2013/2014, which was the driest year with a higher annual average of 17 (Fig. 2). However, precipitation and, consequently, soil water content (SWC) differed among years. The hydrological year 2009/2010 was the rainiest year with a remarkable 535 mm of total precipitation, while 2013/2014 was the driest with 113 mm. During the rest of the study period, annual precipitation ranged from 219 to 296 mm. Generally, most of the precipitation occurs during November-May resulting in the highest values of SWC over the year (Fig. 2), and coinciding with the lowest values of T_{air} and β.

Despite the large variability in annual precipitation over the study period, large CO_2 release was measured in Amoladeras (Fig. 3), even during the rainiest year 2009/2010. The annual cumulative CO_2 release in Amoladeras was on average 231 ± 48 g C m^{-2} year^{-1}. In this regard, the driest year (2013/2014), when annual precipitation was 42% lower than the mean precipitation over the study period, corresponded to the highest amount of CO_2 released to the atmosphere (324 g C m^{-2} year^{-1}; Fig. 4e). Similarly, the lowest annual cumulative CO_2 releases were registered in the rainiest years of the study period: 2012/2013 and 2009/2010 had releases of 163 and 185 g C m^{-2} year^{-1} and annual precipitation of 296 and 535 mm, respectively (Fig. 4d and a, respectively).

Differences among years depend on the length and strength of the net CO_2 uptake observed during the growing season, which was determined by the magnitude and timing of precipitation. For example, during 2009–2012, when rainfall events occurred in both autumn and winter months, although not always evenly distributed, Amoladeras acted as a net CO_2 sink during several months (Fig. 4a–c). In contrast, during the remaining years, net CO_2 uptake occurred during just one winter month (Fig. 4d–f). Concretely, in 2012/2013 and 2014/2015, rainfall was very low or absent in December and January but some precipitation events occurred during autumn and early spring (Fig. 4d and f). In 2013/2014, which was the driest year, very low-magnitude precipitation events were registered (Fig. 4e). Generally, large amounts of CO_2 were released from Amoladeras during late spring, summer and early autumn (i.e. from April–May to November–December), with the exception of 2012/2013, when the CO_2 balance remained almost unchanged from February to June (Fig. 4d).

3.2. Seasonal and diurnal net CO_2 exchange variability

As expected, we found distinct meteorological conditions over growing and dry seasons (Table 2). In general, air and soil temperature, vapor pressure deficit and net radiation (T_{air}, T_{soil}, VPD and R_n, respectively) were lower during the growing season, while precipitation (P) and SWC were considerably higher, compared to the dry season (Table 2). The meteorological variable with the greatest variability among years is precipitation, for both the growing and dry seasons (coefficient of variation, CV, of 44 and 82%, respectively; Table 2). The season length also varied from year to year, with 2012/2013 and 2013/2014 having the longest growing and dry season, respectively (Table 2). In addition, the growing

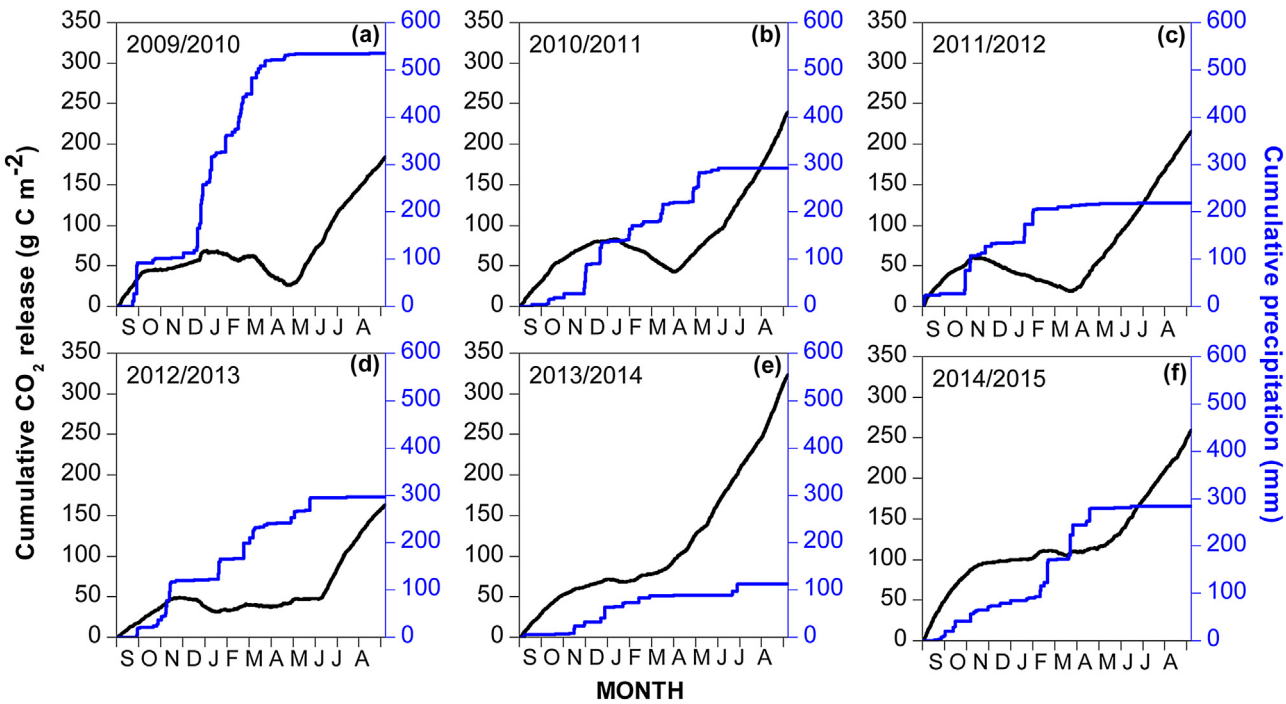

Fig. 4. Cumulative CO_2 release (black line) and precipitation (blue line) for every hydrological year over the study period. (For interpretation of the references to colour in this figure legend, the reader is referred to the web version of this article.)

Table 2
Daily mean values of air and soil temperature (T_{air} and T_{soil}, respectively), soil water content, vapor pressure deficit (VPD) and net radiation (R_n), and sums of precipitation (P), evapotranspiration (ET) and net C emission during growing and dry seasons for each hydrological year (2009–2015). Coefficients of variation (CV; %) for each variable are also shown.

Growing season	Length (days)	T_{air} (°C)	T_{soil} (°C)	SWC ($m^3\,m^{-3}$)	VPD (hPa)	R_n ($W\,m^{-2}$)	P (mm)	ET (mm)	Net CO_2 release ($g\,C\,m^{-2}$)
2009/2010	236	16 ± 4	17 ± 6	0.30 ± 0.19	6 ± 4	48 ± 44	523	208 ± 62	21 ± 7
2010/2011	220	15 ± 4	16 ± 6	0.17 ± 0.07	6 ± 3	56 ± 52	290	188 ± 53	45 ± 5
2011/2012	172	14 ± 5	15 ± 7	0.16 ± 0.06	6 ± 3	34 ± 44	213	122 ± 5	−1 ± 6
2012/2013	240	15 ± 3	16 ± 5	0.14 ± 0.05	6 ± 2	57 ± 52	295	179 ± 51	28 ± 4
2013/2014	140	14 ± 4	14 ± 6	0.12 ± 0.03	6 ± 2	38 ± 43	107	67 ± 26	53 ± 3
2014/2015	226	15 ± 4	16 ± 5	0.13 ± 0.03	6 ± 3	49 ± 42	282	156 ± 5	78 ± 5
CV (%)	18	4	5	35	4	18	44	31	67
Dry season	**Length (days)**	**T_{air} (°C)**	**T_{soil} (°C)**	**SWC ($m^3\,m^{-3}$)**	**VPD (hPa)**	**R_n ($W\,m^{-2}$)**	**P (mm)**	**ET (mm)**	**Net CO_2 release ($g\,C\,m^{-2}$)**
2009/2010	129	23 ± 4	33 ± 4	0.06 ± 0.02	11 ± 5	130 ± 25	12	40 ± 19	163 ± 6
2010/2011	145	23 ± 4	32 ± 6	0.06 ± 0.01	11 ± 4	111 ± 39	2	39 ± 19	195 ± 6
2011/2012	194	21 ± 5	27 ± 6	0.07 ± 0.02	9 ± 4	102 ± 94	6	54 ± 3	218 ± 8
2012/2013	125	23 ± 4	30 ± 6	0.06 ± 0.02	12 ± 6	113 ± 31	1	35 ± 25	135 ± 5
2013/2014	225	21 ± 4	26 ± 5	0.07 ± 0.01	10 ± 4	107 ± 37	6	48 ± 22	271 ± 8
2014/2015	139	24 ± 4	32 ± 5	0.06 ± 0.01	13 ± 6	121 ± 29	1	41 ± 2	182 ± 7
CV (%)	23	6	8	9	14	8	82	15	22

season cumulative net CO_2 exchange was only negative (i.e. net CO_2 uptake) in 2011/2012, with releases of less than 80 g CO_2 m^{-2} for the other years (Table 2). In contrast, dry season cumulative net CO_2 exchange was always above 130 g CO_2 m^{-2} and showed lower inter-annual variability (CV = 22%) than that observed over the growing season (CV = 67%; Table 2).

Accordingly, diurnal patterns of net CO_2 fluxes (F_c) revealed noticeable differences between growing and dry season ecosystem behavior (Fig. 5). In general, during the growing season, maximum net CO_2 uptake occurred in the early morning (i.e. 8–10 AM) for all hydrological years and after that, uptake began to decrease and the ecosystem became neutral or even released CO_2 in the late afternoon (i.e. 4–6 PM; Fig. 5a). Occasionally, in 2013/2014 and 2014/2015, the ecosystem started to release CO_2 up to a peak observed at 1–3 pm (Fig. 5a). In contrast, over the dry season, F_c diurnal patterns were much more symmetric showing a maximum net CO_2 release at around 1 PM (Fig. 5b), but also, similar to growing season patterns, the ecosystem showed slight CO_2 uptake or neutral CO_2 balance at dawn. Regarding nighttime patterns, although there was net CO_2 release during both growing and dry seasons, emission fluxes are subtly higher during the growing season over the whole study period.

Although the general net CO_2 exchange behavior for every season is similar over the study period, some differences among hydrological years were found (Fig. 5). For instance, the maximum daytime net CO_2 uptake (ca. −2 μmol m^{-2} s^{-1}) and maximum nighttime net CO_2 emission (ca. 0.6 μmol m^{-2} s^{-1}) occurred during the growing season of 2009/2010, the year when water availability was the highest (Fig. 5a; Table 2). In addition, growing season F_c patterns of 2009/2010, 2011/2012 and 2012/2013 showed net CO_2 uptake rates during most of the daytime hours (Fig. 5a). However, in the remaining years (i.e. 2010/2011, 2013/2014 and 2014/2015), CO_2 release was measured after 10 am (Fig. 5a). In fact, a symmetric release pattern is noticeable for 2013/2014 and 2014/2015 curves.

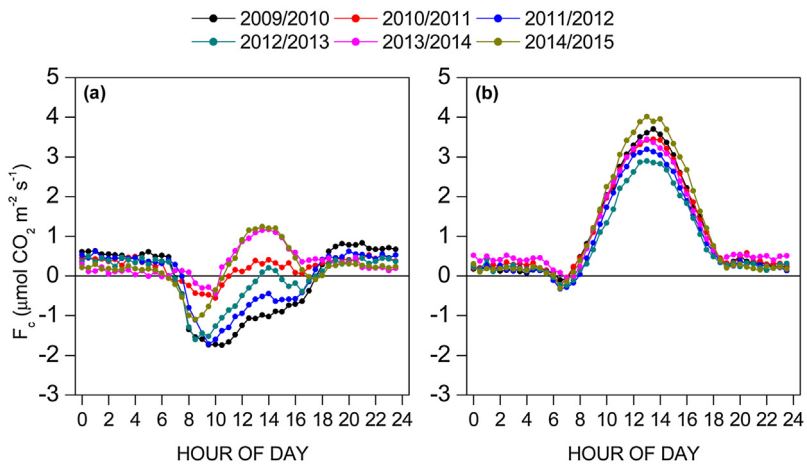

Fig. 5. Averaged diurnal patterns of net CO_2 fluxes over: (a) the growing season and (b) dry season, for every hydrological year over the study period in Amoladeras. Half-hourly CO_2 flux data correspond to non-gapfilled and maximum quality fluxes. (For interpretation of the references to colour in this figure legend, the reader is referred to the web version of this article.)

Table 3
Michaelis-Menten light curve fit parameters (value and error) for every hydrological year over the study period: gross primary production at infinite light (GPP_{max}; $\mu mol\ m^{-2}\ s^{-1}$), level of photosynthetic photon flux density at which net CO_2 flux is half of GPP_{max} (k; $\mu mol\ m^{-2}\ s^{-1}$) and daytime ecosystem respiration (R_d; $\mu mol\ m^{-2}\ s^{-1}$). Adjusted R-squared is also shown and asterisk denotes *p*-value < 0.05. Daytime half-hourly net CO_2 fluxes used for curve fitting are those corresponding to vapor pressure deficit equal or lower than 4 hPa and friction velocity below 0.3 m s-1. Empty space denotes no fit convergence.

Year	n	GPP_{max}		k		R_d		
		Value	Error	Value	Error	Value	Error	Adj. R^2
2009–2010	126	−9.28	7.55	1469.94	2162.88	−0.45	0.70	0.25
2010–2011	54	−4.28	5.17	813.93	2471.14	−0.49	1.17	0.11
2011–2012	82	−4.24*	1.97	511.62	638.24	−0.91	0.52	0.27
2012–2013	87	−4.05	2.58	557.47	916.57	−0.86	0.67	0.16
2013–2014	38	−7.60	6.59	1082.08	1082.08	0.09	0.71	0.37
2014–2015	–	–	–	–	–	–	–	–

Related to the dry season diurnal patterns, the highest release peak of ca. 4 $\mu mol\ m^{-2}\ s^{-1}$ occurred in 2014/2015, while the lowest was observed in 2012/2013 (less than 3 $\mu mol\ m^{-2}\ s^{-1}$; Fig. 5b). Nonetheless, the net CO_2 exchange over the drought period showed considerably less variability among years compared to the growing season patterns.

3.3. Biological and non-biological processes composing the net CO_2 exchange

Regarding biological processes composing the net CO_2 exchange, growing season data were analyzed with the aim to explore ecosystem photosynthesis and respiration. In the case of ecosystem respiration, we found no significant relationship between half-hourly nighttime F_c and T_{soil} for any hydrological year (data not shown). Hence, we centered our analysis on photosynthesis via light curve fitting. Our results show that net CO_2 uptake was affected by VPD, since half-hourly daytime F_c were more related to the photosynthetic photon flux density (PPFD) when VPD was at or below 4 hPa (Fig. 6). In fact, when PPFD and VPD were maximal, net CO_2 release fluxes were observed (i.e. positive daytime half-hourly F_c; Fig. 6). Likewise, we found that net CO_2 release occured when u_* was approximately above 0.45 m s^{-1}, while net CO_2 uptake corresponded to lower u_* values (Fig. 7).

Therefore, only data corresponding to lower water stress and turbulence conditions (VPD ≤ 4 hPa and u_* < 0.3 m s^{-1}) were used to fit the rectangular hyperbolic model (Eq. (1)). Although the fitting procedure was not successful for the last hydrological year (2014/2015; Table 3), we obtained non-linear fit coefficients for the other years. Fitting parameters of maximum gross primary productivity (GPP_{max}) ranged from 4.05 to 9.28 $\mu mol\ m^{-2}\ s^{-1}$, and daytime ecosystem respiration (R_d) was often positive but not significant (p-value > 0.05), since the parameter error exceeded the parameter values for all years (Table 3). Finally, the best fit with significant GPP_{max} coefficient was obtained in 2011/2012 (Adj. R^2 = 0.27; Table 3).

Table 4
Fit parameters (intercept, slope, and R-squared) obtained via linear regression between daytime half-hourly net CO_2 fluxes ($\mu mol\ m^{-2}\ s^{-1}$) and friction velocity (m s^{-1}) when vapor pressure deficit is above 4 hPa over the growing season in Amoladeras. Half-hourly net CO_2 flux data correspond to non-gapfilled and maximum quality fluxes. Data corresponding to rainfall events are excluded. Asterisk denotes *p*-values < 0.05.

Year	n	Intercept	Slope	R^2
2009–2010	1688	0.53*	1.12*	0.05*
2010–2011	2710	−0.1*	3.26*	0.25*
2011–2012	926	1.08*	1.16*	0.02*
2012–2013	3021	−0.04	2.11*	0.15*
2013–2014	1457	0.03	3.08*	0.14*
2014–2015	2286	−0.37*	2.76*	0.13*
All years	12088	0.39*	2.22*	0.10*

To look at non-biological processes, we delved into subterranean ventilation by means of the net CO_2 fluxes (F_c) and the relationship with the friction velocity (u_*) over both growing and dry season. We found a significant linear relationship (p-value < 0.05) between u_* and daytime half-hourly F_c for VPD > 4 hPa, over the growing seasons of all hydrological years (R^2 = 0.10; Table 4). The variance explained by u_* increased to 25% in 2010/2011, and reached its minimum in 2009/2010 and 2011/2012 (R^2 = 0.05 and R^2 = 0.02, respectively), and most of the fit parameters obtained for every year were significant (p-value < 0.05). We

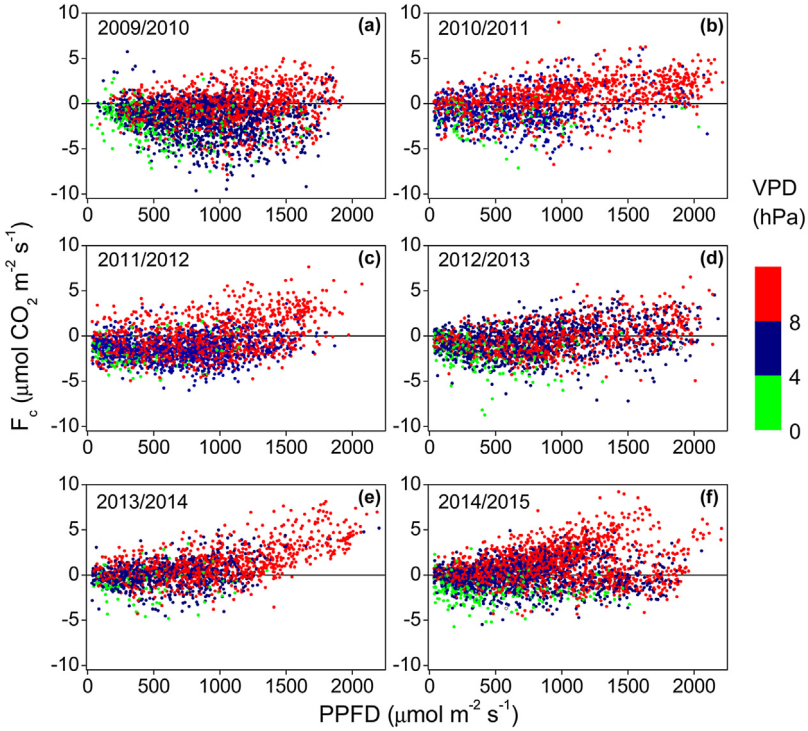

Fig. 6. Light response curves of daytime half-hourly net CO_2 fluxes (F_c) at different levels of vapor pressure deficit (VPD), corresponding to the growing season of each hydrological year over the study period in Amoladeras. Half-hourly F_c data correspond to non-gapfilled and maximum quality fluxes. (For interpretation of the references to colour in this figure legend, the reader is referred to the web version of this article.)

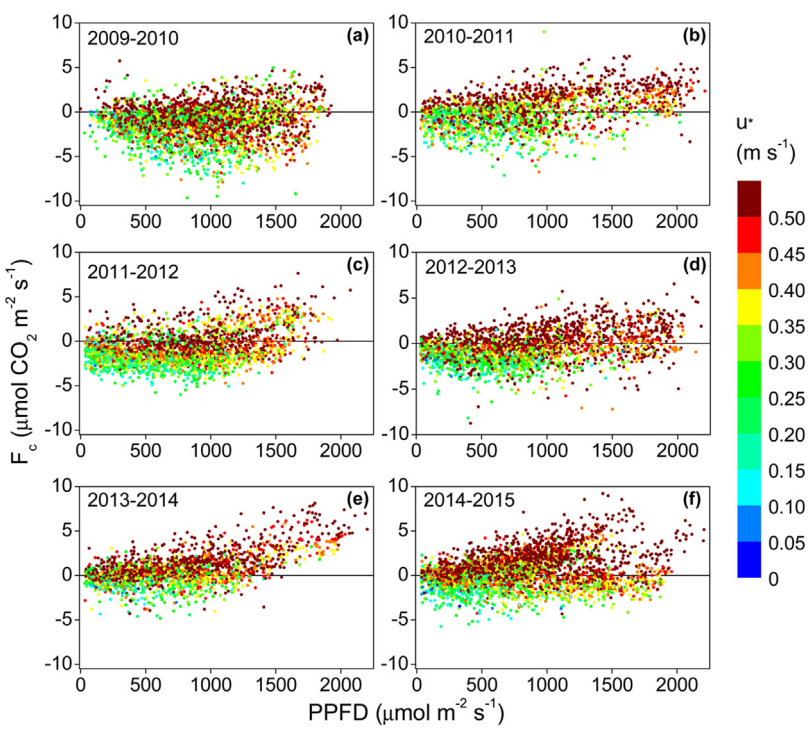

Fig. 7. Light response curves of daytime half-hourly net CO_2 fluxes at different levels of friction velocity (u_*), corresponding to the growing season of each hydrological year over the study period in Amoladeras. Half-hourly F_c data correspond to non-gapfilled and maximum quality fluxes. (For interpretation of the references to colour in this figure legend, the reader is referred to the web version of this article.)

also examined the influence of u_* on F_c fluxes over the dry season, but taking into account the influence of R_n (Fig. 8). Based on the fit parameters obtained, a significant linear relationship was found at the three levels of R_n used and for all hydrological years (p-value < 0.05; Fig. 8). Moreover, the highest R_n level ($R_n > 470\,W\,m^{-2}$) had the best linear fit for 2009/2010 and 2011/2012 data ($R^2 = 0.68$ and 0.59, respectively; Fig. 8a and c) and even when pooling dry season data together ($R^2 = 0.41$; data not

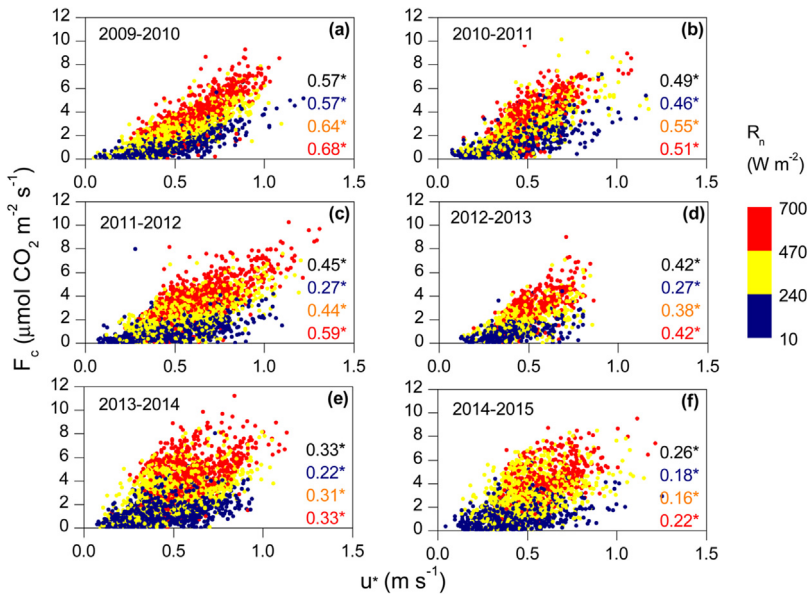

Fig. 8. Relationship between daytime half-hourly net CO_2 fluxes (F_c) and friction velocity (u_*) together with the coefficient of determination (R^2) for every simple linear regression performed at low (dark blue), intermediate (yellow), high (red) and the whole daytime range (black) of net radiation (R_n) levels. Asterisk denotes *p*-values <0.05. Data used correspond to the dry season of each hydrological year in Amoladeras. Half-hourly F_c data correspond to non-gapfilled and maximum quality fluxes excluding rainfall events. (For interpretation of the references to colour in this figure legend, the reader is referred to the web version of this article.)

shown). However, in the cases of 2012/2013 and 2013/2014, variance explained by u_* at the highest level of R_n (R^2 = 0.42 and 0.33, respectively; Fig. 8d and e) was equivalent to that obtained by using the whole range of daytime R_n values (R_n > 10 W m^{-2}), and even, in 2014/2015, the fit was better when using all daytime R_n values (R^2 = 0.26; Fig. 8f). Finally, 2010/2011 was unusual since data showed the best linear fit (R^2 = 0.55; Fig. 8b) at the intermediate R_n level (240 < R_n ≤ 470 W m^{-2}).

3.4. Subsoil CO_2 molar fractions

Regarding CO_2 measurements within the vadose zone, we found that subsoil CO_2 molar fraction at 1.5 m was, on average, 180% higher than that measured at 0.15 m over the 2014/2015 hydrological year (Fig. 9). In addition, differing patterns were also observed between depths; while CO_2 peaked during March and April at 0.15 m (ca. 1500 ppm; Fig. 9a), maximum CO_2 molar fraction was observed from June to October at 1.5 m (ca. 2500; Fig. 9b). Apart from that, sustained medium-high CO_2 values were observed during summer months at the shallowest depth despite the lowest SWC registered, and there was more variability at 0.15 m than at 1.5 m (Fig. 9).

4. Discussion

Our study site, Amoladeras, is located in the driest part of Europe and is part of the 33% of global land area covered by (semi-)arid ecosystems (Okin, 2001). In the present study, we have found very large CO_2 release over the whole study period (2009–2015), averaging 230 g CO_2 m^{-2} year^{-1}, which is far higher than those reported in the literature. Among the available CO_2 balance data measured in water-limited ecosystems with similar precipitation regimes, the maximum values of annual cumulative CO_2 emission measured by EC systems are frequently near or below 150 g CO_2 m^{-2} year^{-1} (Mielnick et al., 2005; Rey et al., 2012a, 2012b; Scott et al., 2015). The extreme CO_2 release observed in Amoladeras, exceeding 300 g CO_2 m^{-2} year^{-1} in 2013/2014, are likely inconsistent with variations of organic carbon pools within this ecosystem (Schlesinger, 2016). In this regard, the soil organic C (SOC) pool in Amoladeras, where soil is 10 cm deep on average, equates to ~1.24 kg C m^{-2}, according to Amoladerasí published soil data (Rey et al., 2011). However, only 20% (~250 g C m^{-2}, maximum) of this SOC would be accessible to microorganisms (Aranda and Oyonarte, 2005; Oyonarte et al., 2007) and hence susceptible to respiratory CO_2 emission. This value is very similar to the annual averaged CO_2 release measured in Amoladeras (230 g CO_2 m^{-2} year^{-1}), which leads us to think that other non-local C sources should be involved in the measured net CO_2 exchange. Otherwise, based on our measurements, this CO_2 release would result in total depletion of SOC pool in a few years.

In fact, the largest CO_2 releases occurred during the driest months which, in turn, support the idea that these fluxes cannot be related to concurrent *in situ* respiration, mainly because, as is widely-known, hydric stress inhibits any biological activity (Huxman et al., 2004). Furthermore, we did not find clear temperature-dependence of night-time net CO_2 fluxes, and the application of the light-response model did not succeed for most of the years of study (Table 3). Rather, sustained subsoil CO_2 molar fractions are observed at 0.15 m depth over dry season despite the high temperatures and low water availability (Fig. 9a), and even, at 1.5 m, maximum CO_2 values coincided with summer months (Fig. 9b). Additionally, CO_2 molar fractions increased with depth, in accordance with what Amundson and Davidson (1990) observed in several ecosystems distributed globally. Accordingly, we hypothesize that two possible origins may be behind this extreme CO_2 release.

On one hand, the first hypothesis supposes a geological origin of the released CO_2, as a direct supply of geologic CO_2 gas from the underlying area near the experimental site. This would correspond, based on Kerrick (2001), to mantle-derived CO_2 from either subaerial dormant volcanos – since Amoladeras is situated near the Cabo de Gata volcanic complex where the last volcanic activity dates to 7.5 million of years ago (Braga-Alarcón et al., 2003) – or to subaerial non-volcanic CO_2 degassing, which has been associated with geothermal systems, seismicity and fault zones, among others. In this regard, the Carboneras Fault Zone crosses near the field site (see Appendix A in Supplementary material), which could entail seismicity and CO_2 degassing (Kerrick, 2001), as proposed

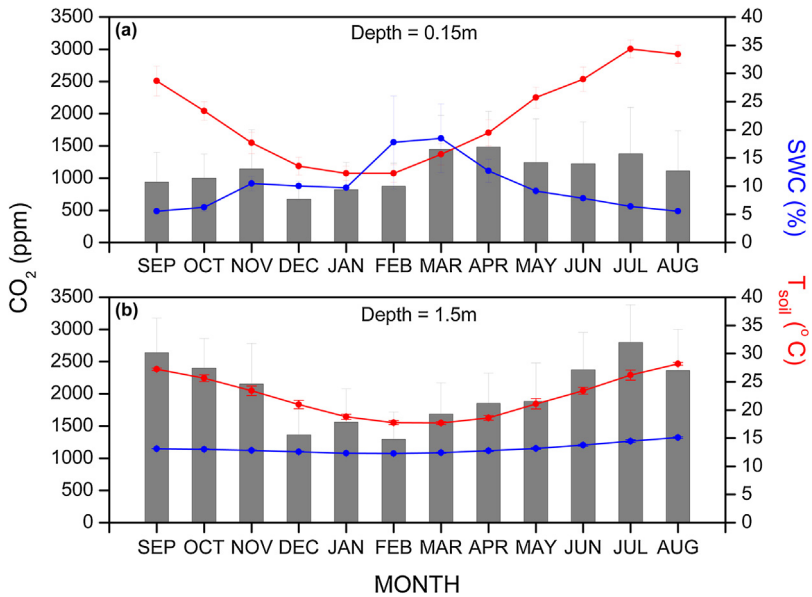

Fig. 9. Monthly averages of subsurface CO_2 (grey bars), volumetric soil water content (SWC; blue lines) and soil temperature (T_{soil}; red lines) at (a) 0.15 m and (b) 1.5 m depths over the hydrological year of 2014/2015. (For interpretation of the references to colour in this figure legend, the reader is referred to the web version of this article.)

by Rey et al. (2012b). This could even act as a conduit facilitating the escape of deep CO_2 (Kerrick, 2001), occasionally via advective transport (i.e. subterranean ventilation; Covington, 2016). However, recognizing that spatial heterogeneity of CO_2 content in the vadose could not be completely assessed with two sensors, the subsoil CO_2 concentrations at 0.15 m and 1.5 m equate to 0.11 and 0.20%, respectively, which are similar to those measured by Rey et al. (2012b) but much lower values than those measured in typical high-temperature magmatic gases and low-temperature hydrothermal gases (0.5–12%; Fischer and Chiodini, 2015). Similarly, CO_2 contents are usually higher in karstic ecosystems, as shown by Sánchez-Cañete et al. (2016) in a Mediterranean shrubland where a similar experimental design was installed.

On the other hand, we hypothesize that subterranean air and water movement could be responsible for CO_2 recharge below the site. The topographic and geological characteristics of Amoladeras are consistent with this theory, since our experimental site is situated within an alluvial basin filled with high permeability sediment (Kerrick, 2001) and is surrounded by terrain at higher altitudes. Additionally, there is an aquifer system (Fig. 10a) where groundwater moves down gradient towards the southwest and Amoladeras (Fig. 10b; Junta de Andalucía, 2013). In this context, we suggest that the CO_2 in both aqueous and gaseous phases is translocated from nearby areas such as Sierra Alhamilla (to the NW) – where belowground CO_2 production can be related to geothermal (Cerón et al., 2000; Rey et al., 2012b) and/or to biological activity given the higher water-availability and milder temperatures, compared to Amoladeras – through the vadose and saturated zones. Within the saturated zone, this transport occurs due to the gradient in the hydraulic head; similarly, a gradient exists in the vadose zone because, like water, CO_2-rich air is denser than atmospheric air (Sánchez-Cañete et al., 2013b). Hence, both gradients establish a downhill pressure gradient force (Fig. 11). Therefore, as suggested by Li et al. (2015), there might be an accumulation of CO_2 under arid basins, but this CO_2 can occasionally escape to the atmosphere via subterranean ventilation, strongly affecting the C balance as proposed by Bourges et al. (2012).

In this regard, based on our results, we suggest that the main process behind this large CO_2 release is subterranean ventilation, which should be conceived as a non-diffusive mass transport process that can be detectable by EC systems under specific conditions. Firstly, the air located in the vadose zone must be significantly CO_2-rich; secondly, soil pores must have low water content to allow gas flow; and thirdly, high turbulence conditions are indispensable to penetrate the soil and transfer the CO_2-rich air from the vadose zone to the atmosphere. We found all these conditions in Amoladeras, especially during the dry season. This leads us to conclude that ventilation played a large role in the sizeable CO_2 release at the site, as also suggested by other studies developed in nearby ecosystems (Kowalski et al., 2008; Rey et al., 2012a,b; Sanchez-Cañete et al., 2011; Serrano-Ortiz et al., 2009). Accordingly, we avoided the widely used terms of Net Ecosystem Carbon Balance (NECB) or Net Ecosystem Exchange (NEE) to refer to the net CO_2 exchange we measured because the released CO_2 is probably not exclusively local and because part of the vadose zone is actually beyond the ecosystem conceptual boundaries (Chapin et al., 2006). We suggest that Amoladeras may be considered as a surface through which the CO_2 accumulated within the vadose zone can be transported to the atmosphere.

Consequently, although some of our results over the growing season indicate photosynthetic activity in Amoladeras (Fig. 5a), the application of the ecophysiological models commonly used to quantify the light and temperature dependencies of net CO_2 fluxes (Fc) did not work well in our case (Table 3), as observed also by Kowalski et al. (2008). In fact, over the growing period of most years, the cumulative CO_2 balance was positive (Table 2) and CO_2 releases were registered at high turbulence and VPD conditions (Figs. 6 and 7). In contrast, during the dry season, ventilative fluxes were much more evident especially during daytime when symmetric CO_2 release patterns were measured for all hydrological years (Fig. 5b), similar to a nearby karstic Mediterranean shrubland (Serrano-Ortiz et al., 2009). In addition, the proportion of F_c variance explained by u_* was greater over the dry season (Fig. 8), and even though regression results were generally better at higher R_n levels this is probably due to the strength of solar heating, which is an important mechanism that triggers turbulence (Stull, 1988). Thus, similar to what Rey et al. (2012a,b) proposed, we suggest that the higher R_n values registered in summer (Table 2) may result in higher convective energy of eddies that could penetrate the water-free soil pores of the deep vadose zone, where CO_2 molar fractions are higher (Fig. 9), and displace the stored CO_2-rich air to the atmosphere. Conversely, at nighttime, atmospheric stability, water

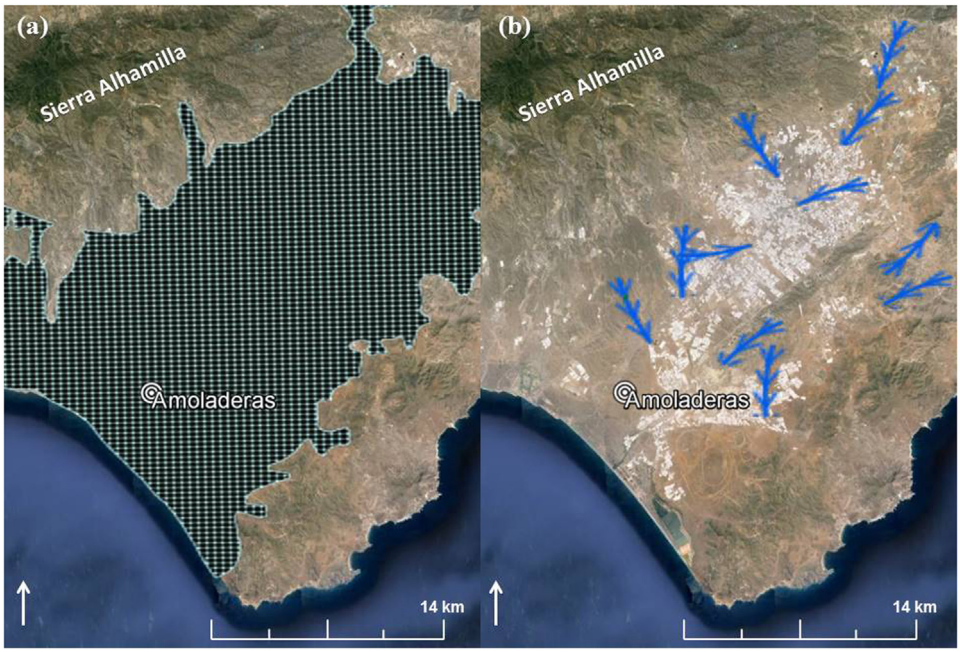

Fig. 10. Hydrogeological characteristics of Amoladeras and surrounding areas: (a) Detritic aquifer system (black-dotted surface) and (b) subterranean water flux paths (blue arrows). (For interpretation of the references to colour in this figure legend, the reader is referred to the web version of this article.)
Source: Mapa de información general de aguas subterráneas de Andalucía (Junta de Andalucía, 2013).

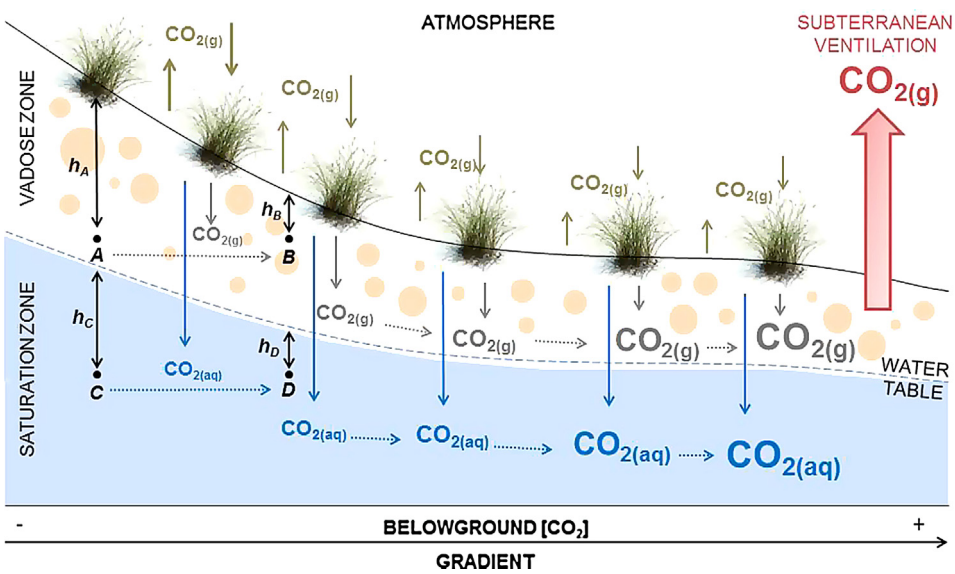

Fig. 11. Diagram describing the lateral and vertical movement of aqueous and gaseous CO_2 above and below the surface. At point C, the hydraulic head is higher than at point D. Similarly, at point A, the head of CO_2-rich air is higher than at point B. Within the vadose and saturation zones, respectively, these heads force air and water flow to the right, towards lower altitudes.

deposition (i.e., dew) and vapor adsorption near the soil surface may inhibit ventilation, as suggested by several studies (Cuezva et al., 2011; Kowalski et al., 2008; Roland et al., 2013; Sanchez-Cañete et al., 2011) since over the dry season relative humidity peaks and u_* reaches its minimum at nighttime hours (data not shown) in Amoladeras. In fact, in a nearby experimental site (13 km far), dewfall represented from 9% to 23% of annual rainfall over 2007–2010 (Uclés et al., 2014).

Overall, our study highlights the relevance of subterranean ventilation as an advective transport process that may affect drylands' C balance, especially under dry and high-turbulence conditions. Additionally, based on our results, we suggest that the large amount of ventilated CO_2 cannot be derived from concurrent, *in situ* respiration. Therefore, we hypothesize, based on published literature, that potential origins of the released CO_2 can be either direct geological degassing or subterranean translocation of CO_2 in both gaseous and aqueous phases, or both. However, future research is needed in order to understand how CO_2 transport and production processes interact and modulate the C balance of semiarid and arid regions. Some future steps could be to determine CO_2 content and isotopic signal of belowground air and water in Amoladeras but also through an altitudinal gradient in order to detect the CO_2 translocation. Additionally, it would be very helpful to accurately locate fractures and fissures within the study area. Finally, in

addition to effects on photosynthesis and respiration of heatwaves and dry spells (Reichstein et al., 2013), the present study demonstrates that such climate extremes can provoke great CO_2 release via subterranean ventilation. This transport process should become more relevant with global warming and associated aridification (Gao and Giorgi, 2008), and furthermore represents a positive feedback to climate change.

Acknowledgements

A. López-Ballesteros acknowledges support from the Spanish Ministry of Economy and Competitiveness [FPI grant, BES-2012-054835]. This work was supported in part by the Spanish Ministry of Economy and Competitiveness projects ICOS-SPAIN [AIC10-A-000474], SOILPROF [CGL2011-15276-E], GEISpain [CGL2014-52838-C2-1-R], including European Union ERDF funds; and by the European Commission project DIESEL [PEOPLE-2013-IOF-625988]. We also thank L. Luquot, J. Benavente and C. Oyonarte for the interesting discussions that improved this paper and L. Morillas, O. Uclés, E. Arnau and R. Moya for field work.

Supplementary data

Supplementary data associated with this article can be found, in the online version, at http://dx.doi.org/10.1016/j.agrformet.2016.12.021.

References

Ahlström, A., Raupach, M.R., Schurgers, G., et al., 2015. The dominant role of semi-arid ecosystems in the trend and variability of the land CO_2 sink. Science 348, 895–899.
Amundson, R.G., Davidson, E.A., 1990. Carbon dioxide and nitrogenous gases in the soil atmosphere. J. Geochem Explor. 38, 13–41.
Aranda, V., Oyonarte, C., 2005. Effect of vegetation with different evolution degree on soil organic matter in a semi-arid environment (Cabo de Gata-Níjar Natural Park, SE Spain). J. Arid Environ. 62, 631–647.
Baena-Pérez, J., Voermans, F., Ruiz Reig, P., 1977. Mapa Geológico de España 1:50,000, Hoja 1045. Instituto Geológico y Minero de España. (IGME).
Bourges, F., Genthon, P., Genty, D., Mangin, A., D'hulst, D., 2012. Comment on Carbon uptake by karsts in the Houzhai Basin, southwest China by Junhua Yan et al. J. Geophys. Res.: Biogeosci. 117 (n/a-n/a).
Bowling, D.R., Massman, W.J., 2011. Persistent wind-induced enhancement of diffusive CO_2 transport in a mountain forest snowpack. J. Geophys. Res.: Biogeosci. 116.
Braga-Alarcón, J.C., Baena, J., Calaforra, J., 2003. The Almeria-Nijar basin. In: Villalobos, M. (Ed.), Geology of the Arid Zone of Almeria (SE Spain). Regional Ministry of Environment and State Water Company for the Southern Basin SA (ACUSUR).
Brandt, L.A., Bonnet, C., King, J.Y., 2009. Photochemically induced carbon dioxide production as a mechanism for carbon loss from plant litter in arid ecosystems. J. Geophys. Res.: Biogeosci. 114.
Carrasco A. (1988) Hidrogeología del Campo de Níjar y acuíferos «marginales» (Almería). TIAC'88, II: 1-36.
Cerón, J.C., Martín-Vallejo, M., García-Rosell, L., 2000. CO_2-rich thermomineral groundwater in the Betic Cordilleras, southeastern Spain: genesis and tectonic implications. Hydrol. J. 8, 209–217.
Chapin, F.S., Woodwell, G.M., Randerson, J.T., 2006. Reconciling carbon-cycle concepts, terminology, and methods. Ecosystems 9, 1041–1050.
Comas, X., Slater, L., Reeve, A., 2007. In situ monitoring of free-phase gas accumulation and release in peatlands using ground penetrating radar (GPR). Geophys. Res. Lett. 34, L06402.
Comas, X., Slater, L., Reeve, A.S., 2011. Atmospheric pressure drives changes in the vertical distribution of biogenic free-phase gas in a northern peatland. J. Geophys. Res.: Biogeosci. 116, G04014.
Covington, M.D., 2016. 8. The importance of advection for CO_2 dynamics in the karst critical zone: an approach from dimensional analysis. Geol. Soc. Am. Spec. Pap. 516, 113–127.
Cuezva, S., Fernandez-Cortes, A., Benavente, D., Serrano-Ortiz, P., Kowalski, A.S., Sanchez-Moral, S., 2011. Short-term CO_2(g) exchange between a shallow karstic cavity and the external atmosphere during summer: role of the surface soil layer. Atmos. Environ. 45, 1418–1427.
Junta de Andalucía, Consejería de Medio Ambiente y Ordenación del Territorio (2013) Mapa de información general de aguas subterráneas de Andalucía. Red de Información Ambiental de Andalucía (REDIAM).
Dlugokencky, E., Tans, P., 2014. Trends in Atmospheric Carbon Dioxide. National Oceanic & Atmospheric Administration, Earth System Research Laboratory (NOAA/ESRL), available at: http://www.esrl.noaa.gov/gmd/ccgg/trends.
Emmerich, W.E., 2003. Carbon dioxide fluxes in a semiarid environment with high carbonate soils. Agric. Forest Meteorol. 116, 91–102.
Fischer, T.B., Chiodini, G., 2015. Volcanic, magmatic and hydrothermal gases. In: Sigurdsson, H., et al. (Eds.), The Encyclopedia of Volcanoes. Elsevier.
Frisia, S., Fairchild, I.J., Fohlmeister, J., Miorandi, R., Spötl, C., Borsato, A., 2011. Carbon mass-balance modelling and carbon isotope exchange processes in dynamic caves. Geochim. Cosmochim. Acta 75, 380–400.
Fujiyoshi, R., Haraki, Y., Sumiyoshi, T., Amano, H., Kobal, I., Vaupotič, J., 2009. Tracing the sources of gaseous components (222Rn, CO2 and its carbon isotopes) in soil air under a cool-deciduous stand in Sapporo, Japan. Environ. Geochem. Health 32, 73–82.
Gao, X., Giorgi, F., 2008. Increased aridity in the Mediterranean region under greenhouse gas forcing estimated from high resolution simulations with a regional climate model. Global Planet. Change 62, 195–209.
Hamerlynck, E.P., Scott, R.L., Sánchez-Cañete, E.P., Barron-Gafford, G.A., 2013. Nocturnal soil CO_2 uptake and its relationship to subsurface soil and ecosystem carbon fluxes in a Chihuahuan Desert shrubland. J. Geophys. Res. G: Biogeosci. 118, 1593–1603.
Hirsch, A.I., Trumbore, S.E., Goulden, M.L., 2004. The surface CO_2 gradient and pore-space storage flux in a high-porosity litter layer Tellus. Ser. B: Chem. Phys. Meteorol. 56, 312–321.
Huxman, T.E., Snyder, K.A., Tissue, D., 2004. Precipitation pulses and carbon fluxes in semiarid and arid ecosystems. Oecologia 141, 254–268.
Joos, F., Spahni, R., 2008. Rates of change in natural and anthropogenic radiative forcing over the past 20,000 years. Proc. Natl. Acad. Sci. U. S. A. 105, 1425–1430.
Kerrick, D.M., 2001. Present and past nonanthropogenic CO_2 degassing from the solid earth. Rev. Geophys. 39, 565–585.
Kowalski, A.S., Serrano-Ortiz, P., Janssens, I.A., 2008. Can flux tower research neglect geochemical CO2 exchange? Agric. Forest Meteorol. 148, 1045–1054.
López-Ballesteros, A., Serrano-Ortiz, P., Sánchez-Cañete, E.P., Oyonarte, C., Kowalski, A.S., Pérez-Priego, Ó., Domingo, F., 2016. Enhancement of the net CO2 release of a semiarid grassland in SE Spain by rain pulses. J. Geophys. Res.: Biogeosci. 121, 2015JG003091.
Le Quéré, C., Raupach, M.R., Canadell, J.G., 2009. Trends in the sources and sinks of carbon dioxide. Nat. Geosci. 2, 831–836.
Li, Y., Wang, Y.G., Houghton, R.A., Tang, L.S., 2015. Hidden carbon sink beneath desert. Geophys. Res. Lett. 42, 5880–5887.
Maier, M., Schack-Kirchner, H., Hildebrand, E.E., Holst, J., 2010. Pore-space CO2 dynamics in a deep, well-aerated soil. Eur. J. Soil Sci. 61, 877–887.
Maier, M., Schack-Kirchner, H., Aubinet, M., Goffin, S., Longdoz, B., Parent, F., 2012. Turbulence effect on gas transport in three contrasting forest soils. Soil Sci. Soc. Am. J. 76, 1518–1528.
Mauder, M., Foken, T., 2004. Documentation and instruction manual of the eddy-covariance software package324 TK3. Abt. Mikrometeorol. 46, 60.
Metcalfe, D.B., 2014. Climate science: a sink down under. Nature 509, 566–567.
Michaelis, L., Menten, M.L., 1913. Die Kinetik der Invertinwirkung. Biochem. Z. 49, 333–369.
Mielnick, P., Dugas, W.A., Mitchell, K., Havstad, K., 2005. Long-term measurements of CO2 flux and evapotranspiration in a Chihuahuan desert grassland. J. Arid Environ. 60, 423–436.
Moncrieff, J.B., Massheder, J.M., De Bruin, H., et al., 1997. A system to measure surface fluxes of momentum, sensible heat, water vapour and carbon dioxide. J. Hydrol. 188–189, 589–611.
Moro, M.J., Were, A., Villagarcía, L., Cantón, Y., Domingo, F., 2007. Dew measurement by Eddy covariance and wetness sensor in a semiarid ecosystem of SE Spain. J. Hydrol. 335, 295–302.
Okin, G.S., 2001. Wind-driven Desertification: Process Modeling, Remote Monitoring, and Forecasting, PhD Thesis. California Institute of Technology, Pasadena California.
Oyonarte, C., Mingorance, M.D., Durante, P., Piñero, G., Barahona, E., 2007. Indicators of change in the organic matter in arid soils. Sci. Total Environ. 378, 133–137.
Pérez-Priego, O., Serrano-Ortiz, P., Sánchez-Cañete, E.P., Domingo, F., Kowalski, A.S., 2013. Isolating the effect of subterranean ventilation on CO2 emissions from drylands to the atmosphere. Agric. Forest Meteorol. 180, 194–202.
Poulter, B., Frank, D., Ciais, P., 2014. Contribution of semi-arid ecosystems to interannual variability of the global carbon cycle. Nature 509, 600–603.
Redeker, K.R., Baird, A.J., Teh, Y.A., 2015. Quantifying wind and pressure effects on trace gas fluxes across the soil?atmosphere interface. Biogeosciences 12, 7423–7434.
Reichstein, M., Falge, E., Baldocchi, D., 2005. On the separation of net ecosystem exchange into assimilation and ecosystem respiration: review and improved algorithm. Global Change Biol. 11, 1424–1439.
Reichstein, M., Bahn, M., Ciais, P., 2013. Climate extremes and the carbon cycle. Nature 500, 287–295.
Rey, A., Pegoraro, E., Oyonarte, C., Were, A., Escribano, P., Raimundo, J., 2011. Impact of land degradation on soil respiration in a steppe (Stipa tenacissima L.) semi-arid ecosystem in the SE of Spain. Soil Biol. Biochem. 43, 393–403.
Rey, A., Belelli-Marchesini, L., Were, A., et al., 2012a. Wind as a main driver of the net ecosystem carbon balance of a semiarid Mediterranean steppe in the South East of Spain. Global Change Biol. 18, 539–554.
Rey, A., Etiope, G., Belelli-Marchesini, L., Papale, D., Valentini, R., 2012b. Geologic carbon sources may confound ecosystem carbon balance estimates: evidence

from a semiarid steppe in the southeast of Spain. J. Geophys. Res.: Biogeosci. 117, G03034, http://dx.doi.org/10.1029/2012JG001991.
Rey, A., Belelli-Marchesini, L., Etiope, G., Papale, D., Canfora, E., Valentini, R., Pegoraro, E., 2013. Partitioning the net ecosystem carbon balance of a semiarid steppe into biological and geological components. Biogeochemistry 118, 83, http://dx.doi.org/10.1007/s10533-013-9907-4.
Roland, M., Serrano-Ortiz, P., Kowalski, A.S., 2013. Atmospheric turbulence triggers pronounced diel pattern in karst carbonate geochemistry. Biogeosciences 10, 5009–5017.
Rutledge, S., Campbell, D.I., Baldocchi, D., Schipper, L.A., 2010. Photodegradation leads to increased carbon dioxide losses from terrestrial organic matter. Global Change Biol. 16, 3065–3074.
Rutter, E.H., Faulkner, D.R., Burgess, R., 2012. Structure and geological history of the Carboneras fault zone, SE Spain: part of a stretching transform fault system. J. Struct. Geol. 45, 68–86.
Sánchez-Cañete, E.P., Kowalski, A.S., Serrano-Ortiz, P., Pérez-Priego, O., Domingo, F., 2013a. Deep CO2 soil inhalation/exhalation induced by synoptic pressure changes and atmospheric tides in a carbonated semiarid steppe. Biogeosciences 10, 6591–6600.
Sánchez-Cañete, E.P., Serrano-Ortiz, P., Domingo, F., Kowalski, A.S., 2013b. Cave ventilation is influenced by variations in the CO2-dependent virtual temperature. Int. J. Speleol. 42, 1–8.
Sánchez-Cañete, E.P., Oyonarte, C., Serrano-Ortiz, P., Curiel Yuste, J., Pérez-Priego, O., Domingo, F., Kowalski, A.S., 2016. Winds induce CO2 exchange with the atmosphere and vadose zone transport in a karstic ecosystem. J. Geophys. Res.: Biogeosci. 121, 2049–2063.
Sanchez-Cañete, E.P., Serrano-Ortiz, P., Kowalski, A.S., Oyonarte, C., Domingo, F., 2011. Subterranean CO2 ventilation and its role in the net ecosystem carbon balance of a karstic shrubland. Geophys. Res. Lett., 38.
Schlesinger, W.H., 1990. Evidence from chronosequence studies for a low carbon-storage potential of soils. Nature 348, 232–234.
Schlesinger, W.H., 2016. An evaluation of abiotic carbon sinks in deserts. Global Change Biol., n/a-n/a.
Scott, R.L., Biederman, J.A., Hamerlynck, E.P., Barron-Gafford, G.A., 2015. The carbon balance pivot point of southwestern U.S. semiarid ecosystems: insights from the 21 st century drought. J. Geophys. Res.: Biogeosci. 120, 2612–2624.
Seok, B., Helmig, D., Williams, M.W., Liptzin, D., Chowanski, K., Hueber, J., 2009. An automated system for continuous measurements of trace gas fluxes through snow: an evaluation of the gas diffusion method at a subalpine forest site, Niwot Ridge, Colorado. Biogeochemistry 95, 95–113.
Serrano-Ortiz, P., Domingo, F., Cazorla, A., 2009. Interannual CO_2 exchange of a sparse Mediterranean shrubland on a carbonaceous substrate. J. Geophys. Res. G: Biogeosci. 114.
Serrano-Ortiz, P., Roland, M., Sanchez-Moral, S., Janssens, I.A., Domingo, F., Goddéris, Y., Kowalski, A.S., 2010. Hidden, abiotic CO_2 flows and gaseous reservoirs in the terrestrial carbon cycle: review and perspectives. Agric. Forest Meteorol. 150, 321–329.
Serrano-Ortiz, P., Sánchez-Cañete, E.P., Oyonarte, C., 2012. The carbon cycle in drylands. In: Lal, R., et al. (Eds.), Recarbonization of the Biosphere. Springer-Verlag, New York.
Stull, R.B., 1988. An Introduction to Boundary Layer Meteorology. Kluwer Academic Publishers, Dordrecht.
Subke, J.-A., Reichstein, M., Tenhunen, J.D., 2003. Explaining temporal variation in soil CO2 efflux in a mature spruce forest in Southern Germany. Soil Biol. Biochem. 35, 1467–1483.
Takle, E.S., Massman, W.J., Brandle, J.R., 2004. Influence of high-frequency ambient pressure pumping on carbon dioxide efflux from soil. Agric. Forest Meteorol. 124, 193–206.
Uclés, O., Villagarcía, L., Moro, M.J., Canton, Y., Domingo, F., 2014. Role of dewfall in the water balance of a semiarid coastal steppe ecosystem. Hydrol. Processes 28, 2271–2280.
Weijermars, R., 1991. Geology and tectonics of the Betic zone, SE Spain. Earth Sci. Rev. 31, 153–236.
Wilson, K., et al., 2002. Energy balance closure at FLUXNET sites. Agric. For. Meteorol. 113 (1-4), 223–243.
World Reference Base for Soil Resources, 2006. World Soil Resources Reports 103. FAO, Rome, Italy.